CD27 an emerging immuno-oncology target at the cross-roads of innate and adaptive anti-tumor immune responses

KINETA®
Kineta Inc. 219 Terry Av. North, Seattle, WA 98109
tguillaudeux@kineta.us

AACR #A60

Shawn Iadonato, Jessica Cross, Nathan Eyde, Emily Frazier, Neda Kabi, Chen Katz, Remington Lance, Kurt Lustig, Yulia Ovechkina, David Peckham, Shaarwari Sridhar, Carla Talbaux, Isabelle Tihista, Mei Xu, and Thierry Guillaudeux

Introduction

- CD27 is a member of the TNF-Receptor superfamily expressed on CD4+ and CD8+ T cells, on NK and NKT cells and on B cells,
- CD27 promotes T cell co-activation, proliferation, clonal expansion and differentiation into antigen specific cytotoxic and memory T cells after stimulation with its ligand CD70,
- The costimulatory signal of CD27 on T cells is mediated via the NFkB pathway but also via the phosphatidylinositol 3 kinase and the protein kinase B pathways,
- CD27 signaling influences the innate immune response via direct activation of NK cells and a subsequent secretion of interferon-gamma (IFN-γ),
- CD27 plays a central role in immunological responses and by promoting T cell and NK cell activation it contributes to anti-tumor immunity,
- Kineta generated a library of 147 fully human anti-CD27 monoclonal antibodies after immunization of Trianni mice and selected a lead candidate with strong agonistic proprieties (T. Guillaudeux, et al. Cancer Res 2022;82(12_Suppl): 4261).

Objectives

- Determine anti-CD27 antibody affinity to human CD27,
- Evaluate anti-CD27 antibody cross-reactivity to human, non-human primate and murine CD27,
- Assess anti-CD27 antibody agonistic activity using NFkB-Luc2/CD27 Jurkat reporter assay,
- Characterize the stimulatory effects of the anti-CD27 antibody on human T and NK cells,
- Evaluate the anti-tumor efficacy of our lead antibody as a single agent *in vivo*.

Anti-CD27 antibody leads bind hCD27 with high affinity

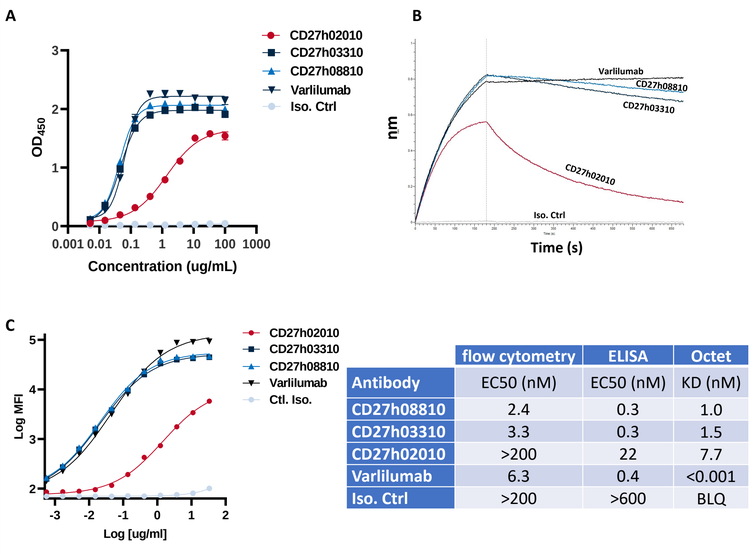

Antibody	flow cytometry EC50 (nM)	ELISA EC50 (nM)	Octet KD (nM)
CD27h08810	2.4	0.3	1.0
CD27h03310	3.3	0.3	1.5
CD27h02010	>200	22	7.7
Varlilumab	6.3	0.4	<0.001
Iso. Ctrl	>200	>600	BLQ

Figure 1. (A) ELISA binding studies were conducted with immobilized human CD27 (rabbit-Fc). Binding of anti-CD27 antibodies was detected using biotinylated anti-human IgG (light chain) followed by streptavidin HRP. (B) Kinetics sensorgrams of anti-CD27 antibodies and immobilized human CD27. Fitted association and dissociation curves generated using Octet (FortéBio, Sartorius AG). Kinetic studies were performed in PBS, 0.02% BSA, 0.002% Tween 20, pH 7.2 buffer using hCD27-ECD-His-tag loaded onto HIS1K dip and read biosensors. A 1:1 global curve fitting analysis was performed to determine equilibrium (KD), association (ka) and dissociation (kdis) rate constants. BLQ stands for below the limit of quantification. (C) The Alexa Fluor 647 conjugated anti-CD27 antibodies were evaluated for binding to hCD27-Flp-In-CHO cells using Attune Nxt Flow Cytometry. Data was analyzed using log MFI (mean fluorescence intensity).

Results

Anti-CD27 antibody leads bind specifically to human and cynomolgus monkey CD27

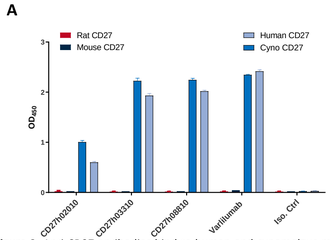

B

Antibody	Human CD27 KD (nM)	Cynomolgus CD27 KD (nM)	Mouse CD27 KD (nM)
CD27h08810	1.0	1.9	BLQ
CD27h03310	1.5	2.3	BLQ
CD27h02010	7.7	11	BLQ
Varlilumab	<0.001	<0.001	BLQ
Ctl. Iso	BLQ	BLQ	BLQ

Figure 2. Anti-CD27 antibodies bind to human and cynomolgus monkey CD27 similarly while no binding is observed for the rat and mouse CD27 (A) Binding of anti-CD27 antibodies to immobilized human CD27 (rabbit-Fc), cynomolgus monkey CD27 (human-Fc), rat CD27 (mouse-Fc) or mouse CD27 (mouse-Fc) measured by ELISA. Bound anti-CD27 antibodies were detected using biotinylated anti-human IgG (light chain) followed by streptavidin HRP. Error bars represent SD (standard deviation). (B) Kinetics sensorgrams of anti-CD27 antibodies and immobilized human, cynomolgus monkey or mouse CD27. Fitted association and dissociation curves generated using Octet (FortéBio, Sartorius AG). Kinetic studies were performed in PBS, 0.02% BSA, 0.002% Tween 20, pH 7.2 buffer using CD27-ECD-His-tag loaded onto HIS1K dip and read biosensors. A 1:1 global curve fitting analysis was performed to determine equilibrium (KD), association (ka) and dissociation (kdis) rate constants. BLQ stands for below the limit of quantification.

Anti-CD27 antibody leads show high on-target specificity

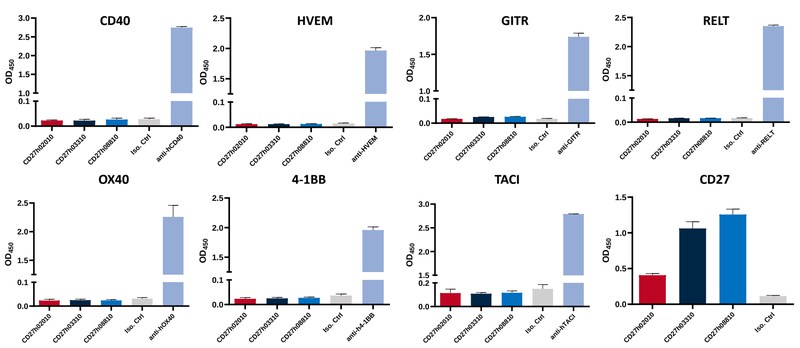

Figure 3. Binding of anti-CD27 antibodies to immobilized human TNFRSF proteins measured by ELISA. Bound anti-CD27 antibodies were detected using biotinylated anti-human IgG (light chain) followed by streptavidin HRP. Error bars represent SD (standard deviation).

Anti-CD27 antibody leads induce NFκB-mediated CD27 signaling in soluble format

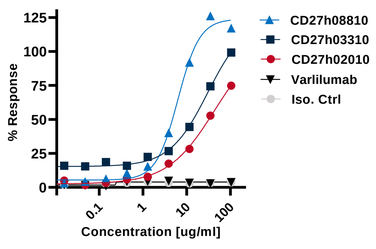

	EC50 (μg/mL)	EC50 (nM)
CD27h08810	7.2	49
CD27h03310	18	123
CD27h02010	33	226
Varlilumab	>104	>714
Iso. Ctrl	>104	>713

Figure 4. Anti-CD27 agonistic antibody assay was carried out with NFκB-Luc2/CD27 Jurkat cells in X-VIVO-15 medium in the 96-well plates pre-coated with 5 μg/mL anti-CD3 mAb. Cells were incubated with anti-CD27 antibodies for 4 hrs at 37ºC, 5% CO2 humidified incubator. NFkB reporter induction was measured by luminescence in the presence of Bio-Glo reagent.

Anti-CD27 antibody leads activate NK cells

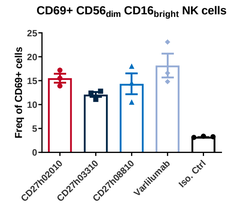

Figure 5: PBMCs from healthy donors were cultured with 10 μg/mL of anti-CD27 antibodies. Cells were harvested after 96 hours, stained with fixable live dead dye and surface markers for NK cells, fixed with BD cytofix buffer and analyzed using Attune Nxt Flow Cytometry. After doublet and dead cell discrimination, CD56dim CD16bright cells were evaluated for activation marker CD69. Graphical representation of frequency of CD69+ cells in CD56dim CD16bright cells is shown. Error bars represent SEM.

Anti-CD27 antibody leads activate T cells

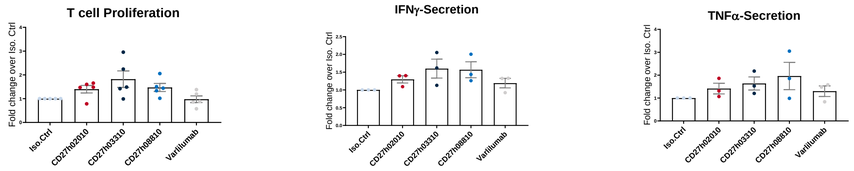

Figure 6. Effect of anti-CD27 antibodies on T cell proliferation and cytokine secretion. The human pan T-cells were labeled with CellTrace™ Violet dye and cultured using 1μg/mL anti-CD3 (OKT3) coated plates in the presence of 5μg/mL canti-CD28 soluble antibody and 10 μg/mL anti-CD27 antibodies for 96 hours. T cell proliferation was quantified using Attune Nxt Flow Cytometry. The IFNγ and TNFα secretion was quantified by Milliplex Map Kit Human Cytokine/Chemokine/Growth Factor Panel A (Millipore) using Luminex MAGPIX. The average of fold change over isotype control antibody (Iso. Ctrl) was calculated for five healthy donors. Error bars represent SEM.

Anti-CD27 antibody leads demonstrate *in vivo* anti-tumor efficacy

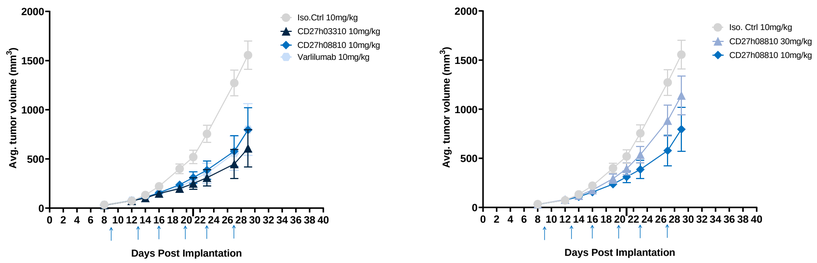

Figure 7. Plot of the average tumor volumes vs. time following subcutaneous implantation of 1x10^6 Raji cells/mouse into female NOD-SCID mice. Nine days after cell implantation, mice received IP injection of 10 mg/kg of isotype control antibody (Iso. Ctrl), 10 mg/kg of CD27h03310, 10 mg/kg or 30 mg/kg of CD27h08810, or 10 mg/kg of Varlilumab. All antibodies were administered twice a week for 3 weeks (as indicated by arrows). Error bars represent SEM.

Conclusions

- We selected the lead therapeutic antibody from our library of 147 fully human anti-CD27 monoclonal antibodies generated in the Trianni mice,
- We confirmed our lead antibodies' binding potency and cross-reactivity with human and cynomolgus monkey CD27 but not with the murine CD27,
- Our antibody leads demonstrated strong agonist proprieties on T cell proliferation and activation after engagement of NFκB as well as NK cell activation,
- Our lead antibody is currently evaluated as a single agent or in combination with other immuno-therapies *in vivo* in solid and hematological mouse tumor models in hCD27-KI mice.